

Angular-dependent matrix potentials for fast molecular-dynamics simulations of transition metals

This article has been downloaded from IOPscience. Please scroll down to see the full text article.

2006 J. Phys.: Condens. Matter 18 S447

(<http://iopscience.iop.org/0953-8984/18/16/S06>)

View [the table of contents for this issue](#), or go to the [journal homepage](#) for more

Download details:

IP Address: 129.252.86.83

The article was downloaded on 28/05/2010 at 10:07

Please note that [terms and conditions apply](#).

Angular-dependent matrix potentials for fast molecular-dynamics simulations of transition metals

S L Dudarev

EURATOM/UKAEA Fusion Association, Culham Science Centre, Oxfordshire OX14 3DB, UK

Received 15 August 2005, in final form 6 February 2006

Published 3 April 2006

Online at stacks.iop.org/JPhysCM/18/S447

Abstract

The significance of the part played by the angular-dependent components of forces associated with d–d bonding between atoms in a transition metal has long remained a subject of debate. While almost all the large-scale molecular dynamics simulations of collision cascades and radiation damage in transition metals and alloys are currently performed using spherically symmetric many-body potentials, density functional calculations exhibit a highly anisotropic pattern of charge density deformation in and around the core of interstitial atom defects. This paper describes a fast second-order matrix recursion-based algorithm for including effects of angular anisotropy of d–d bonds in a large-scale molecular dynamics simulation.

1. Introduction

The development of semi-empirical interatomic potentials for simulating defect structures in transition metals and alloys has recently attracted considerable attention in the field of fusion and advanced nuclear materials [1, 2]. Modelling interaction of energetic neutrons and ions with steels and other transition metal alloys requires using potentials suitable for simulating systems containing in excess of a hundred thousand atoms. Systems of this size are well beyond the reach of the currently available density functional or tight-binding electronic-structure-based approaches that can only treat configurations containing no more than ~ 1000 atoms. Hence the overwhelming majority of large-scale molecular-dynamics simulations performed today are based on the semi-empirical many-body potentials of the Finnis–Sinclair [3–5] or the embedded atom model (EAM) [6] type where interaction between atoms is described by a combination of relatively simple radial functions of atomic coordinates.

Until a few years ago the form of these radial functions was determined by fitting to the observed values of elastic constants and to the equation of state of the material. However, density functional studies of interstitial and vacancy defects [7–10] showed that semi-empirical potentials constructed in this way were not sufficiently accurate in describing the relative energies of defects and defect migration pathways. Owing to this difficulty, the more recent strategy in the development of interatomic potentials has focused on fitting a potential,

still taken in its spherically symmetric form, to a more complete input data set including, for example, energies of formation of interstitial and vacancy defects found using density functional calculations [11, 12]. The resulting potentials have relatively long range, sometimes extending far beyond the second coordination cell of atoms in the bcc lattice. At the same time, the possible effect of angular-dependent forces on the structure and energies of defects in a transition metal has not been explored.

What is the logic behind describing interatomic interactions in a transition metal by a spherically symmetric function? Since the atomic d orbitals responsible for this interaction have strong angular character, it is natural to expect the occurrence of angular-dependent terms in the expression for interatomic forces. Carlsson [13], Kress and Voter [14], and Foiles [15] investigated this point numerically using a model where every atom in a transition metal had exactly five d electrons, and concluded that in this particular case interatomic interactions were well approximated by spherically symmetric functions. While in the particular case of a half-filled d band this conclusion agrees with the analysis given below, it does not seem to agree with the recent density functional calculations showing strong anisotropy of charge density deformations in the core of interstitial defects [10]. Hence the main argument in favour of choosing the spherically symmetric functional form of a many-body second-order potential is not its fundamental validity, but rather its convenience, simplicity and low computational cost.

Directional interatomic forces are currently investigated in connection with structural stability of transition metals and intermetallic compounds [16, 17], where it is believed that only the higher order terms (associated with the fourth and the sixth order moments of the density of states) contain information about the angular character of d–d bonds. There is only one recent study, carried out by Krasko *et al* [18], where the effect of angular forces on interatomic interaction in iron was addressed. Krasko *et al* assumed that the angular terms had the same functional form as those in the Tersoff potential for silicon. Since the angular symmetry of d–d bonds differs from that of s–p bonds, it is unlikely that this approximation provides a fundamentally consistent starting point for the treatment of interatomic forces in a transition metal.

In this paper we address two questions. Firstly, what is the contribution of angular terms to energies and forces *at the second-moment level of approximation* in the case where the number of d electrons per atom is not equal to five? Secondly, is there a *practical* algorithm for carrying out a large-scale molecular dynamics simulation if the angular terms are included?

Both questions focus mainly on the methodology of a simulation. The significance of posing these questions comes from the fact that at present the selection of interatomic potentials suitable for a large-scale molecular dynamics simulation is still very limited. In the case of a transition metal system there is still no sufficiently simple *and* logically consistent approach that would allow taking angular terms into account at a low computational cost. This paper presents a full derivation of a method capable of taking angular terms into account, and gives a working example showing that the method can be used to reproduce more accurately the energies of interstitial defect structures, and to study large-scale collision cascades only accessible at present to simulations performed using spherically symmetric potentials.

The method is based on the second-order matrix (or block) recursion approximation. The difference between the scalar and the matrix recursion algorithms consists in that the latter provides a way of evaluating the elements of the on-site Green's function and the on-site density of states for the case where the initial composite state for recursion is *degenerate* [19, 20]. This point is significant for developing a consistent treatment of interaction between transition metal atoms since it is the subspace of five degenerate d orbitals that forms the initial state for recursion. Finding the spectrum of eigenvalues and eigenstates of a matrix recursion solution for the Green's function requires diagonalizing a circular matrix similarly to the perturbation

treatment of a multiplet of degenerate states [21]. Hence a matrix-recursion-based molecular-dynamics algorithm not only provides a way of treating angular interatomic forces, it also introduces an essentially quantum mechanical element in a molecular dynamics simulation. Surprisingly, this does not substantially increase the computational cost of the algorithm, and practical simulations can still be performed for systems containing 10^5 or more atoms.

2. The second-level block-recursion approximation

The *scalar* recursion algorithm for evaluating the on-site element of the Green's function $G_{00}(E) = [(E + i0)\hat{I} - \hat{H}]_{00}^{-1}$ uses a special set of basis states (the so-called Lanczos basis set [22]), in which the tight-binding Hamiltonian matrix \hat{H} is tri-diagonal and the Schrödinger operator $E\hat{I} - \hat{H}$ has the form

$$E\hat{I} - \hat{H} = \begin{pmatrix} E - a_0 & -b_1^* & 0 & \cdots \\ -b_1 & E - a_1 & -b_2^* & \cdots \\ 0 & -b_2 & E - a_2 & \cdots \\ \cdots & \cdots & \cdots & \cdots \end{pmatrix}. \quad (1)$$

Both the diagonal a_i and the off-diagonal b_i elements of the Hamiltonian matrix defined in the Lanczos basis are related to the conventional real-space hopping matrix elements $H_{\alpha\beta}$ through a sequence of linear transformations described in [22, 23]. Using the above definition, the 00 on-site element of the inverse matrix $\hat{G}(E) = [(E + i0)\hat{I} - \hat{H}]^{-1}$ can be found using the minor expansion starting from the diagonal element situated in the upper left corner of (1), namely

$$\begin{aligned} G_{00}(E) &= [(E + i0)\hat{I} - \hat{H}]_{00}^{-1} = [E + i0 - a_0 - b_1 G_{11}(E) b_1^*]^{-1} \\ &= \frac{1}{E + i0 - a_0 - \frac{|b_1|^2}{E + i0 - a_1 - \frac{|b_2|^2}{E + i0 - a_2 \cdots}}}. \end{aligned} \quad (2)$$

Here $G_{11}(E)$ is the top diagonal element of the inverse of matrix (1), in which all the elements of the first column and the first row are deleted. By terminating the recursion expansion at the second level we find that $G_{00}(E) = [E + i0 - a_0 - |b_1|^2/(E + i0 - a_1)]^{-1}$. This second-order formula is valid in the case where the initial state of the recursion expansion is non-degenerate.

In the case where the initial state of recursion is a part of a multiplet of degenerate states (as it is in the case of a transition metal atom where the initial state is a part of a fivefold degenerate multiplet of 3d states), it is the entire multiplet of states associated with an atom that has to be treated as a single 'composite' initial state [19, 20]. In this case the simplest second-level recursion expression for the Green's function has the form

$$[\hat{G}_{00}^{-1}(E)]_{ij} = E\delta_{ij} - (i|\hat{H}^\dagger \hat{H}|j)/E, \quad (3)$$

where indices i and j refer to individual orbitals forming the multiplet associated with lattice site 0, and subscript 00 refers to the on-site element of the Green's function. Formula (3) shows that finding the spectrum of $\hat{G}_{00}(E)$ requires diagonalizing the matrix $(i|\hat{H}^\dagger \hat{H}|j)$. The matrix elements of $[\hat{G}_{00}(E)]_{ij}$ can be found using the orthogonal transformation

$$[\hat{G}_{00}(E)]_{ij} = \sum_J C_{iJ} \frac{1}{E + i0 - \mathcal{E}_J^2/(E + i0)} C_{Jj}^\dagger, \quad (4)$$

where the matrix of transformation C_{iJ} consists of eigenvectors of the matrix $\hat{H}^\dagger \hat{H}$, i.e.

$$\mathcal{E}_J^2 \delta_{JJ'} = \sum_{ij} C_{ji}^\dagger (i|\hat{H}^\dagger \hat{H}|j) C_{iJ}. \quad (5)$$

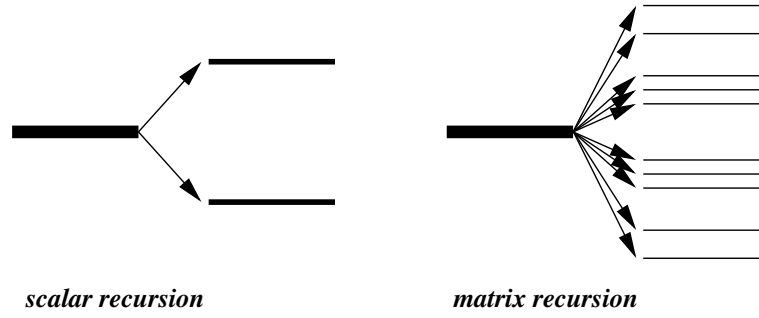


Figure 1. Schematic illustration of the difference between the spectra of states generated by the scalar and the matrix recursion algorithms at the second-moment level of approximation. The process of formation of covalent ‘multi-centred’ d–d bonding and antibonding states eliminates the original degeneracy of the multiplet of atomic d states, and is correctly described in the matrix recursion approximation. At the same level of approximation the scalar recursion approach (equation (2)) gives rise to a spectrum of states consisting of only two levels.

The energy of interaction between an atom occupying site 0 and atoms occupying neighbouring sites is given by the integral over the spectrum $D_{00}(E)$ of the projected on-site density of states

$$\begin{aligned} E_{\text{site } 0} &= 2 \int_{-\infty}^{\epsilon_F} dE E D_{00}(E) = -\frac{2}{\pi} \int_{-\infty}^{\epsilon_F} dE E \sum_j \text{Im}[\hat{G}_{00}^{-1}(E)]_{jj} \\ &= -\frac{2}{\pi} \int_{-\infty}^{\epsilon_F} dE E \text{Im} \sum_{J,j} C_{jJ} \frac{1}{E + i0 - \mathcal{E}_j^2/(E + i0)} C_{jJ}^\dagger, \end{aligned} \quad (6)$$

where the factor of two comes from summation over spin. Using the fact that \hat{C} is orthogonal, i.e. $\sum_j C_{jJ} C_{jJ}^\dagger = 1$, and using the formula $\text{Im}(x + i0)^{-1} = -\pi \delta(x)$, we find that [24, 25]

$$\begin{aligned} E_{\text{site } 0} &= -\frac{2}{\pi} \int_{-\infty}^{\epsilon_F} dE E \text{Im} \sum_J \frac{E}{(E + i0 - |\mathcal{E}_J|)(E + i0 + |\mathcal{E}_J|)} \\ &= -\frac{1}{\pi} \int_{-\infty}^{\epsilon_F} dE E \text{Im} \sum_J \left[\frac{1}{E + i0 - |\mathcal{E}_J|} + \frac{1}{E + i0 + |\mathcal{E}_J|} \right] \\ &= -\sum_J \Theta_J^B |\mathcal{E}_J| + \sum_{J'} \Theta_{J'}^A |\mathcal{E}_{J'}|, \end{aligned} \quad (7)$$

where Θ_J^B and Θ_J^A are the occupation numbers of the local bonding (B) and antibonding (A) states (these states have energies $E = -|\mathcal{E}_J|$ and $E = |\mathcal{E}_J|$, respectively). The states are occupied sequentially starting from the lowest energy bonding state. The local charge neutrality condition [26] imposes a constraint according to which the sum of occupation numbers of bonding and antibonding states must be equal to the total number of electrons on a site. In the case of d electrons the total number of many-body bonding and antibonding states formed as a result of interaction of an atom with its neighbours equals ten. The fact that this is indeed the case is easy to appreciate by considering the example of a diatomic molecule, where a set of d orbitals centred on each atom gives rise, through hybridization, to a set of five bonding and five antibonding states. In a transition metal, application of the second-order matrix recursion to the subspace of five degenerate d orbitals gives rise to the spectrum of states (6) consisting of ten collective multi-centred bonding and antibonding ‘molecular orbital’ levels. The difference between the spectra of states generated by the scalar and the matrix recursion algorithms is illustrated in figure 1.

A practical molecular-dynamics algorithm based on formula (7) has to satisfy two requirements. First, it has to rely on a fast diagonalization algorithm for finding the eigenvalues \mathcal{E}_j^2 of matrix (5) and, second, it has to provide a recipe for evaluating forces acting on atoms. Below we show how both points can be addressed within a single algorithm.

3. The on-site density of states and the total energy

In the original formulation of the second-order matrix recursion approach [13, 14] the matrix elements of $(i|\hat{H}^\dagger\hat{H}|j)$ are evaluated numerically by performing a summation over 3d orbitals associated with every neighbouring atom

$$(i|\hat{H}^\dagger\hat{H}|j) = \sum_k \sum_{\text{nei}} (i, 0|\hat{H}^\dagger|k, \text{nei})(k, \text{nei}|\hat{H}|0, j). \quad (8)$$

Here index k refers to atomic orbitals and ‘nei’ refers to neighbouring atoms. Equation (8) gives rise to a fairly lengthy expression, since each neighbouring atom contributes five terms to the sum. For example, assuming that the starting recursion lattice site has only one neighbour, we find that

$$\begin{aligned} (xy|\hat{H}^\dagger\hat{H}|xy) &= (xy|\hat{H}^\dagger|xy)(xy|\hat{H}|xy) + (xy|\hat{H}^\dagger|yz)(yz|\hat{H}|xy) + (xy|\hat{H}^\dagger|zx)(zx|\hat{H}|xy) \\ &+ (xy|\hat{H}^\dagger|x^2 - y^2)(x^2 - y^2|\hat{H}|xy) + (xy|\hat{H}^\dagger|3z^2 - r^2)(3z^2 - r^2|\hat{H}|xy), \end{aligned} \quad (9)$$

where the $|xy\rangle$ orbital is centred on site 0. Substituting the Slater–Koster formulae [27] for the hopping matrix elements into this equation, we arrive at

$$\begin{aligned} (xy|\hat{H}^\dagger\hat{H}|xy) &= [3l^2m^2(dd\sigma) + (l^2 + m^2 - 4l^2m^2)(dd\pi) + (n^2 + l^2m^2)(dd\delta)]^2 \\ &+ [3lm^2n(dd\sigma) + ln(1 - 4m^2)(dd\pi) + ln(m^2 - 1)(dd\delta)]^2 \\ &+ [3l^2mn(dd\sigma) + mn(1 - 4l^2)(dd\pi) + mn(l^2 - 1)(dd\delta)]^2 \\ &+ \left[\frac{3}{2}lm(l^2 - m^2)(dd\sigma) + 2lm(m^2 - l^2)(dd\pi) + \frac{1}{2}lm(l^2 - m^2)(dd\delta) \right]^2 \\ &+ \left[\sqrt{3}lm[n^2 - \frac{1}{2}(l^2 + m^2)](dd\sigma) - 2\sqrt{3}lmn^2(dd\pi) \right. \\ &\left. + \frac{\sqrt{3}}{2}lm(1 + n^2)(dd\delta) \right]^2, \end{aligned} \quad (10)$$

where l , m and n are direction cosines of the vector pointing from one atom to the other. The 5×5 matrix $(i|\hat{H}^\dagger\hat{H}|j)$ has 15 independent matrix elements analogous to (10). Evaluating forces acting on atoms requires differentiating these matrix elements. Since very lengthy expressions are not convenient for carrying out differentiation, we investigate the possibility of simplifying the above formulae by projecting the starting subspace of orbitals onto another subspace defined in a specially chosen system of coordinates. We write equation (8) in the form

$$\begin{aligned} (i|\hat{H}^\dagger\hat{H}|j) &= \sum_{\text{nei}} [(i, 0|\hat{H}^\dagger|\sigma, \text{nei})(\sigma, \text{nei}|\hat{H}|0, j) \\ &+ (i, 0|\hat{H}^\dagger|\pi_1, \text{nei})(\pi_1, \text{nei}|\hat{H}|0, j) + (i, 0|\hat{H}^\dagger|\pi_2, \text{nei})(\pi_2, \text{nei}|\hat{H}|0, j) \\ &+ (i, 0|\hat{H}^\dagger|\delta_1, \text{nei})(\delta_1, \text{nei}|\hat{H}|0, j) + (i, 0|\hat{H}^\dagger|\delta_2, \text{nei})(\delta_2, \text{nei}|\hat{H}|0, j)], \end{aligned} \quad (11)$$

where the new five 3d orbitals, σ , π_1 , π_2 , δ_1 and δ_2 , are defined in a virtual Cartesian system of coordinates where the z -axis is parallel to the direction of the bond linking the initial recursion lattice site and a neighbouring atom. For example, $|\sigma\rangle$ denotes the $|3z^2 - r^2\rangle$ orbital defined in

the system of coordinates where the z -axis is parallel to the interatomic bond. In the azimuthal and polar angle representation this orbital has the form

$$(\theta, \phi|\sigma) = \sqrt{\frac{5}{16\pi}} [3(\mathbf{e} \cdot \mathbf{v})^2 - 1], \quad (12)$$

where \mathbf{v} is a unit vector in the direction of the bond, and vector \mathbf{e} has components $\mathbf{e} = (\sin\theta \cos\phi, \sin\theta \sin\phi, \cos\theta)$. Similarly, $|\pi_1\rangle$ and $|\pi_2\rangle$ states are the $|zx\rangle$ and $|zy\rangle$ states defined in the above virtual system of coordinates, and $|\delta_1\rangle$ and $|\delta_2\rangle$ states are the corresponding $|xy\rangle$ and $|x^2 - y^2\rangle$ states. Introducing the distance-dependent Slater–Koster coefficients $(dd\sigma) = \{(dd\sigma)(R)\}$, $(dd\pi) = \{(dd\pi)(R)\}$, and $(dd\delta) = \{(dd\delta)(R)\}$, we write

$$\begin{aligned} (i|\hat{H}^\dagger \hat{H}|j) = & \sum_{\text{nei}} [(i, 0|\sigma, 0)(\sigma, 0|0, j)\{(dd\sigma)(R_{\text{nei}})\}^2 \\ & + \{(i, 0|\pi_1, 0)(\pi_1, 0|0, j) + (i, 0|\pi_2, 0)(\pi_2, 0|0, j)\}\{(dd\pi)(R_{\text{nei}})\}^2 \\ & + \{(i, 0|\delta_1, 0)(\delta_1, 0|0, j) + (i, 0|\delta_2, 0)(\delta_2, 0|0, j)\}\{(dd\delta)(R_{\text{nei}})\}^2], \end{aligned} \quad (13)$$

where R_{nei} is the distance between the central atom and its neighbour.

Matrix elements $(i|\hat{H}^\dagger \hat{H}|j)$ can now be readily evaluated by integrating over the solid angle. For example,

$$(3z^2 - r^2, 0|\sigma, 0) = \frac{5}{16\pi} \int d\Omega_{\mathbf{e}} [3(\mathbf{e} \cdot \mathbf{n})^2 - 1] [3(\mathbf{e} \cdot \mathbf{v})^2 - 1] = \frac{1}{2} [3(\mathbf{n} \cdot \mathbf{v})^2 - 1].$$

To perform the integration we use the formulae

$$\begin{aligned} \int d\Omega_{\mathbf{e}} e_i e_j &= \frac{4\pi}{3} \delta_{ij} \\ \int d\Omega_{\mathbf{e}} e_i e_j e_k e_l &= \frac{4\pi}{15} [\delta_{ij}\delta_{kl} + \delta_{ik}\delta_{jl} + \delta_{il}\delta_{jk}], \end{aligned} \quad (14)$$

where $e_i = (e_x, e_y, e_z)$ are the Cartesian components of the unit vector $\mathbf{e} = (\sin\theta \cos\phi, \sin\theta \sin\phi, \cos\theta)$. Using the Slater–Koster notation $l = \mathbf{v}_x = (\mathbf{n}_x \cdot \mathbf{v})$, $m = \mathbf{v}_y = (\mathbf{n}_y \cdot \mathbf{v})$, and $n = \mathbf{v}_z = (\mathbf{n}_z \cdot \mathbf{v})$, and by carrying out the integration, we evaluate all the projections of 3d orbitals defined in the conventional Cartesian system of coordinates onto the set of ‘virtual’ orbitals $|\sigma\rangle$, $|\pi_1\rangle$ and $|\pi_2\rangle$, namely

$$\begin{aligned} (xy|\sigma) &= \sqrt{3}lm, \\ (xz|\sigma) &= \sqrt{3}ln, \\ (yz|\sigma) &= \sqrt{3}mn, \\ (x^2 - y^2|\sigma) &= \frac{\sqrt{3}}{2} (l^2 - m^2), \\ (3z^2 - r^2|\sigma) &= \frac{1}{2} (3n^2 - 1), \end{aligned} \quad (15)$$

and

$$\begin{aligned} (xy|\pi_1) &= (\mathbf{n}_x \cdot \boldsymbol{\lambda}_x)(\mathbf{n}_y \cdot \mathbf{v}) + (\mathbf{n}_y \cdot \boldsymbol{\lambda}_x)(\mathbf{n}_x \cdot \mathbf{v}), \\ (xy|\pi_2) &= (\mathbf{n}_x \cdot \boldsymbol{\lambda}_y)(\mathbf{n}_y \cdot \mathbf{v}) + (\mathbf{n}_y \cdot \boldsymbol{\lambda}_y)(\mathbf{n}_x \cdot \mathbf{v}), \\ (xz|\pi_1) &= (\mathbf{n}_x \cdot \boldsymbol{\lambda}_x)(\mathbf{n}_z \cdot \mathbf{v}) + (\mathbf{n}_z \cdot \boldsymbol{\lambda}_x)(\mathbf{n}_x \cdot \mathbf{v}), \\ (xz|\pi_2) &= (\mathbf{n}_x \cdot \boldsymbol{\lambda}_y)(\mathbf{n}_z \cdot \mathbf{v}) + (\mathbf{n}_z \cdot \boldsymbol{\lambda}_y)(\mathbf{n}_x \cdot \mathbf{v}), \\ (yz|\pi_1) &= (\mathbf{n}_y \cdot \boldsymbol{\lambda}_x)(\mathbf{n}_z \cdot \mathbf{v}) + (\mathbf{n}_z \cdot \boldsymbol{\lambda}_x)(\mathbf{n}_y \cdot \mathbf{v}), \\ (yz|\pi_2) &= (\mathbf{n}_y \cdot \boldsymbol{\lambda}_y)(\mathbf{n}_z \cdot \mathbf{v}) + (\mathbf{n}_z \cdot \boldsymbol{\lambda}_y)(\mathbf{n}_y \cdot \mathbf{v}), \\ (x^2 - y^2|\pi_1) &= (\mathbf{n}_x \cdot \boldsymbol{\lambda}_x)(\mathbf{n}_x \cdot \mathbf{v}) - (\mathbf{n}_y \cdot \boldsymbol{\lambda}_x)(\mathbf{n}_y \cdot \mathbf{v}), \\ (x^2 - y^2|\pi_2) &= (\mathbf{n}_x \cdot \boldsymbol{\lambda}_y)(\mathbf{n}_x \cdot \mathbf{v}) - (\mathbf{n}_y \cdot \boldsymbol{\lambda}_y)(\mathbf{n}_y \cdot \mathbf{v}), \\ (3z^2 - r^2|\pi_1) &= \sqrt{3}(\mathbf{n}_z \cdot \boldsymbol{\lambda}_x)(\mathbf{n}_z \cdot \mathbf{v}), \\ (3z^2 - r^2|\pi_2) &= \sqrt{3}(\mathbf{n}_z \cdot \boldsymbol{\lambda}_y)(\mathbf{n}_z \cdot \mathbf{v}). \end{aligned} \quad (16)$$

Here λ_x and λ_y are the unit vectors of the x and the y axes of the virtual system of coordinates. Using the fact that for any two arbitrarily chosen vectors \mathbf{a} and \mathbf{b} the unit vectors λ_x and λ_y satisfy the equation

$$(\mathbf{a} \cdot \lambda_x)(\mathbf{b} \cdot \lambda_x) + (\mathbf{a} \cdot \lambda_y)(\mathbf{b} \cdot \lambda_y) = (\mathbf{a} \cdot \mathbf{b}) - (\mathbf{a} \cdot \mathbf{v})(\mathbf{b} \cdot \mathbf{v}),$$

we find a simple formula for the matrix element (10)

$$\begin{aligned} (xy|\hat{H}^\dagger\hat{H}|xy) &= (xy|\sigma)(\sigma|xy)(dd\sigma)^2 + [(xy|\pi_1)(\pi_1|xy) + (xy|\pi_2)(\pi_2|xy)](dd\pi)^2 \\ &= 3l^2m^2(dd\sigma)^2 + (dd\pi)^2\{[(\mathbf{n}_x \cdot \lambda_x)(\mathbf{n}_y \cdot \mathbf{v}) + (\mathbf{n}_y \cdot \lambda_x)(\mathbf{n}_x \cdot \mathbf{v})]^2 \\ &\quad + [(\mathbf{n}_x \cdot \lambda_y)(\mathbf{n}_y \cdot \mathbf{v}) + (\mathbf{n}_y \cdot \lambda_y)(\mathbf{n}_x \cdot \mathbf{v})]^2\} \\ &= 3l^2m^2(dd\sigma)^2 + [m^2 + l^2 - 4m^2l^2](dd\pi)^2. \end{aligned} \quad (17)$$

By carrying out similar calculations we evaluate all the 15 independent elements of the matrix $\hat{H}^\dagger\hat{H}$, namely

$$\begin{aligned} (xy|\hat{H}^\dagger\hat{H}|xy) &= 3l^2m^2(dd\sigma)^2 + (l^2 + m^2 - 4l^2m^2)(dd\pi)^2, \\ (xy|\hat{H}^\dagger\hat{H}|yz) &= 3lm^2n(dd\sigma)^2 + ln(1 - 4m^2)(dd\pi)^2, \\ (xy|\hat{H}^\dagger\hat{H}|xz) &= 3l^2mn(dd\sigma)^2 + mn(1 - 4l^2)(dd\pi)^2, \\ (xy|\hat{H}^\dagger\hat{H}|x^2 - y^2) &= \frac{3}{2}lm(l^2 - m^2)(dd\sigma)^2 + 2lm(m^2 - l^2)(dd\pi)^2, \\ (xy|\hat{H}^\dagger\hat{H}|3z^2 - r^2) &= \sqrt{3}lm[n^2 - \frac{1}{2}(l^2 + m^2)](dd\sigma)^2 - 2\sqrt{3}lmn^2(dd\pi)^2, \\ (yz|\hat{H}^\dagger\hat{H}|yz) &= 3m^2n^2(dd\sigma)^2 + (m^2 + n^2 - 4m^2n^2)(dd\pi)^2, \\ (yz|\hat{H}^\dagger\hat{H}|xz) &= 3n^2lm(dd\sigma)^2 + lm(1 - 4n^2)(dd\pi)^2, \\ (yz|\hat{H}^\dagger\hat{H}|x^2 - y^2) &= \frac{3}{2}mn(l^2 - m^2)(dd\sigma)^2 - mn[1 + 2(l^2 - m^2)](dd\pi)^2, \\ (yz|\hat{H}^\dagger\hat{H}|3z^2 - r^2) &= \sqrt{3}mn[n^2 - \frac{1}{2}(l^2 + m^2)](dd\sigma)^2 + \sqrt{3}mn(l^2 + m^2 - n^2)(dd\pi)^2, \\ (xz|\hat{H}^\dagger\hat{H}|xz) &= 3n^2l^2(dd\sigma)^2 + (n^2 + l^2 - 4n^2l^2)(dd\pi)^2, \\ (xz|\hat{H}^\dagger\hat{H}|x^2 - y^2) &= \frac{3}{2}nl(l^2 - m^2)(dd\sigma)^2 + nl[1 - 2(l^2 - m^2)](dd\pi)^2, \\ (xz|\hat{H}^\dagger\hat{H}|3z^2 - r^2) &= \sqrt{3}ln[n^2 - \frac{1}{2}(l^2 + m^2)](dd\sigma)^2 + \sqrt{3}ln(l^2 + m^2 - n^2)(dd\pi)^2, \\ (x^2 - y^2|\hat{H}^\dagger\hat{H}|x^2 - y^2) &= \frac{3}{4}(l^2 - m^2)^2(dd\sigma)^2 + [l^2 + m^2 - (l^2 - m^2)^2](dd\pi)^2, \\ (x^2 - y^2|\hat{H}^\dagger\hat{H}|3z^2 - r^2) &= \frac{\sqrt{3}}{2}(l^2 - m^2)\left[n^2 - \frac{1}{2}(l^2 + m^2)\right](dd\sigma)^2 \\ &\quad + \sqrt{3}n^2(m^2 - l^2)(dd\pi)^2, \\ (3z^2 - r^2|\hat{H}^\dagger\hat{H}|3z^2 - r^2) &= [n^2 - \frac{1}{2}(l^2 + m^2)]^2(dd\sigma)^2 + 3n^2(l^2 + m^2)(dd\pi)^2. \end{aligned} \quad (18)$$

The compact analytical expressions for the matrix elements of $\hat{H}^\dagger\hat{H}$ given above can now be used for numerical programming, as well as for analytical calculations. For example, matrix elements (18) can be readily differentiated *analytically*, providing a way of rapidly evaluating forces acting on atoms.

A more complete list of matrix elements of $\hat{H}^\dagger\hat{H}$, including also the $(dd\delta)$ part of the Slater–Koster overlap integrals, is given in appendix A. Additional matrix elements describing the s–d hybridization effects are given in appendix B.

To find the spectrum of the on-site density of states, matrix elements (18) must now be summed over all the neighbouring lattice sites (see equation (8)) within the range of the Slater–Koster radial functions $\{(dd\sigma)(R)\}$, $\{(dd\pi)(R)\}$ and $\{(dd\delta)(R)\}$. The resulting 5×5 (or 6×6 ,

if the s–d hybridization is included) $\hat{H}^\dagger \hat{H}$ matrix is diagonalized, producing the energies $\mp |\mathcal{E}_J|$ of the local bonding and antibonding states. The total energy of bonds between a given atom and its neighbours is then found by means of equation (7). Finding forces acting on atoms does not require differentiating the eigenstates, and the procedure for finding forces is described in the next section.

4. Forces acting on atoms

In a quantum mechanical treatment, forces acting on atoms are evaluated by means of the Hellmann–Feynman theorem [28]. This theorem is based on the fact that the eigenstates of a Hermitian Hamiltonian operator are orthogonal and normalized, and hence the differentiation of these eigenstates gives no contribution to forces.

A significant difference between the matrix recursion approach and the more conventional quantum mechanical treatment of interatomic forces is that in the matrix recursion approach we diagonalize the *square* of the hopping Hamiltonian matrix rather than the Hamiltonian matrix itself. Hence in the matrix recursion approach the Hellmann–Feynman theorem does not apply.

To evaluate forces we first introduce a notation $D_{ij} = (i|\hat{H}^\dagger \hat{H}|j)$. Equation (5) now has the form

$$\mathcal{E}_J^2 \delta_{JJ'} = \sum_{ij} C_{Ji}^\dagger D_{ij} C_{jJ'}. \quad (19)$$

Assume that matrix D_{ij} is a function of some external parameter ξ , i.e. $D_{ij} = D_{ij}(\xi)$. The eigenvalues and eigenvectors of this matrix are functions of ξ , too, namely

$$\mathcal{E}_J^2(\xi) = \sum_{ij} C_{Ji}^\dagger(\xi) D_{ij}(\xi) C_{jJ}(\xi). \quad (20)$$

To determine how an eigenvalue \mathcal{E}_J^2 varies in response to an infinitesimal variation of parameter ξ , we write

$$\mathcal{E}_J^2(\xi) - \mathcal{E}_J^2(\xi_0) = \sum_{ij} C_{Ji}^\dagger(\xi_0) [D_{ij}(\xi) - D_{ij}(\xi_0)] C_{jJ}(\xi_0). \quad (21)$$

This equation takes into account the fact that the response of the matrix of eigenstates $C_{Ji}(\xi)$ to a small perturbation is of the second order in the perturbation parameter, while the variation of an eigenvalue is linear in the perturbation [21]. In the limit $\xi - \xi_0 \rightarrow 0$ we find that

$$\frac{\partial}{\partial \xi} \mathcal{E}_J^2(\xi) = \sum_{ij} C_{Ji}^\dagger(\xi) \left[\frac{\partial}{\partial \xi} D_{ij}(\xi) \right] C_{jJ}(\xi). \quad (22)$$

This gives rise to a simple formula for the derivative of an eigenstate

$$\frac{\partial}{\partial \xi} \mathcal{E}_J(\xi) = \frac{1}{2\mathcal{E}_J(\xi)} \frac{\partial}{\partial \xi} \mathcal{E}_J^2(\xi) = \mp \frac{\sum_{ij} C_{Ji}^\dagger(\xi) \left[\frac{\partial}{\partial \xi} D_{ij}(\xi) \right] C_{jJ}(\xi)}{2\sqrt{\sum_{ij} C_{Ji}^\dagger(\xi) D_{ij}(\xi) C_{jJ}(\xi)}}, \quad (23)$$

where the minus sign refers to a bonding and the plus sign refers to an antibonding state. In a molecular dynamics simulation we differentiate the eigenstates with respect to the relative position of an atom $\mathbf{R}_{\alpha\beta}$. Hence the force acting on an atom is given by

$$\mathbf{F}_\alpha = \frac{1}{2} \sum_{\beta, \beta \neq \alpha} \sum_J \Theta_J^{(B)} \left\{ \frac{1}{|\mathcal{E}_J(\alpha)|} \sum_{i,j} C_{Ji}^\dagger(\alpha) \left[\frac{\partial}{\partial \mathbf{R}_\alpha} D_{ij}(\mathbf{R}_\alpha - \mathbf{R}_\beta) \right] C_{jJ}(\alpha) \right. \\ \left. + \frac{1}{|\mathcal{E}_J(\beta)|} \sum_{i,j} C_{Ji}^\dagger(\beta) \left[\frac{\partial}{\partial \mathbf{R}_\alpha} D_{ij}(\mathbf{R}_\alpha - \mathbf{R}_\beta) \right] C_{jJ}(\beta) \right\}$$

$$\begin{aligned}
& -\frac{1}{2} \sum_{\beta, \beta \neq \alpha} \sum_{J'} \Theta_{J'}^{(A)} \left\{ \frac{1}{|\mathcal{E}_{J'}(\alpha)|} \sum_{i,j} C_{J'i}^\dagger(\alpha) \left[\frac{\partial}{\partial \mathbf{R}_\alpha} D_{ij}(\mathbf{R}_\alpha - \mathbf{R}_\beta) \right] C_{jJ'}(\alpha) \right. \\
& \left. + \frac{1}{|\mathcal{E}_{J'}(\beta)|} \sum_{i,j} C_{J'i}^\dagger(\beta) \left[\frac{\partial}{\partial \mathbf{R}_\alpha} D_{ij}(\mathbf{R}_\alpha - \mathbf{R}_\beta) \right] C_{jJ'}(\beta) \right\}, \quad (24)
\end{aligned}$$

and summation over J, J' is performed over all the occupied (bonding and antibonding) states.

Formula (24) gives a recipe for evaluating forces acting on atoms in the second-order matrix recursion molecular dynamics algorithm. To find the forces we do not need to differentiate the matrix of eigenstates C_{iJ} , and this reduces the computational cost of the algorithm to a minimum. In practical terms, the only significant difference between a conventional ‘classical’ molecular dynamics algorithm and the matrix recursion algorithm consists in the step involving the diagonalization of a small matrix. The small size of the $\hat{H}^\dagger \hat{H}$ matrix and the fact that equation (24) is not too sensitive to the accuracy of the diagonalization algorithm makes the computational cost of the diagonalization step (19) acceptable for practical large-scale molecular dynamics simulations.

5. Applications of the method

Before discussing applications of the method based on the formalism described above, we investigate the connection between the second-order matrix algorithm and the Finnis–Sinclair approximation [3, 4]. What happens if we average the matrix elements of $\hat{H}^\dagger \hat{H}$ over the solid angle of 4π ? Using the formulae

$$\begin{aligned}
\overline{l^2} &= \overline{m^2} = \overline{n^2} = \frac{1}{3}, \\
\overline{l^4} &= \overline{m^4} = \overline{n^4} = \frac{3}{15}, \\
\overline{l^2 m^2} &= \overline{m^2 n^2} = \overline{n^2 l^2} = \frac{1}{15},
\end{aligned} \quad (25)$$

where

$$\overline{f(\theta, \phi)} = \frac{1}{4\pi} \int d\Omega f(\theta, \phi) = \frac{1}{4\pi} \int_0^{2\pi} d\phi \int_0^\pi \sin\theta d\theta f(\theta, \phi),$$

we find that

$$\overline{(i|\hat{H}^\dagger \hat{H}|j)} = \delta_{ij} \sum_{\text{nei}} \left\{ \frac{1}{5} [(dd\sigma)(R_{\text{nei}})]^2 + \frac{2}{5} [(dd\pi)(R_{\text{nei}})]^2 + \frac{2}{5} [(dd\delta)(R_{\text{nei}})]^2 \right\}. \quad (26)$$

This equation shows that the average of the matrix $\overline{\hat{H}^\dagger \hat{H}}$ is proportional to the unit matrix δ_{ij} , and the pre-factor equals one-fifth of the second moment of the density of states μ_2 given by equation (7.155) of [4].

We note that it follows from equation (13) that the trace of the matrix $\hat{H}^\dagger \hat{H}$

$$\begin{aligned}
\text{Tr}(\hat{H}^\dagger \hat{H}) &= \sum_i (i|\hat{H}^\dagger \hat{H}|i) = \sum_i \sum_{\text{nei}} [(\sigma, 0|0, i)(i, 0|\sigma, 0)\{(dd\sigma)(R_{\text{nei}})\}^2 \\
&\quad + \{(\pi_1, 0|0, i)(i, 0|\pi_1, 0) + (\pi_2, 0|0, i)(i, 0|\pi_2, 0)\}\{(dd\pi)(R_{\text{nei}})\}^2 \\
&\quad + \{(\delta_1, 0|0, i)(i, 0|\delta_1, 0) + (\delta_2, 0|0, i)(i, 0|\delta_2, 0)\}\{(dd\delta)(R_{\text{nei}})\}^2] \\
&= \sum_{\text{nei}} [(\sigma, 0|\sigma, 0)\{(dd\sigma)(R_{\text{nei}})\}^2 \\
&\quad + \{(\pi_1, 0|\pi_1, 0) + (\pi_2, 0|\pi_2, 0)\}\{(dd\pi)(R_{\text{nei}})\}^2 \\
&\quad + \{(\delta_1, 0|\delta_1, 0) + (\delta_2, 0|\delta_2, 0)\}\{(dd\delta)(R_{\text{nei}})\}^2] \\
&= \sum_{\text{nei}} [\{(dd\sigma)(R_{\text{nei}})\}^2 + 2\{(dd\pi)(R_{\text{nei}})\}^2 + 2\{(dd\delta)(R_{\text{nei}})\}^2], \quad (27)
\end{aligned}$$

is also proportional to the second moment of the density of states μ_2 given by equation (7.155) of [4]. Hence the operation of taking the trace of the matrix $(i|\hat{H}^\dagger\hat{H}|j)$ is in some ways equivalent to averaging the matrix elements of $(i|\hat{H}^\dagger\hat{H}|j)$ over the direction of bonds linking an atom to its neighbours. A corollary of this fact is that the matrix

$$\mathcal{D}_{ij} = (i|\hat{H}^\dagger\hat{H}|j) - \overline{(i|\hat{H}^\dagger\hat{H}|j)}, \quad (28)$$

has zero trace, and its elements describe the *net angular-dependent part* of the energy of many-body interaction between atoms in a transition metal.

Furthermore, the fact that the trace of a matrix is invariant with respect to an orthogonal transformation shows that eigenvalues of matrix $(i|\hat{H}^\dagger\hat{H}|j)$ satisfy the condition

$$\sum_{J=1}^5 \mathcal{E}_J^2 = \sum_{\text{nei}} [\{(dd\sigma)(R_{\text{nei}})\}^2 + 2\{(dd\pi)(R_{\text{nei}})\}^2 + 2\{(dd\delta)(R_{\text{nei}})\}^2].$$

This condition implies that in the case of a half-filled band the contribution of angular terms to bonding is a minimum. This justifies the use of the Finnis–Sinclair spherically symmetric form of the many-body potential and explains why Kress and Voter [14], and Carlsson [13] did not find evidence for a significant part being played by angular forces in the case where the number of d electrons per atom was assumed to be equal to five. It is only this special case that was investigated in the past by Carlsson [13] and Foiles [15], as illustrated for example by the use of the trace operator in equation (4) of [13] and in equation (6) of [15]. In the half-filled band case the difference between the total energies evaluated using the matrix and the scalar recursion approaches is relatively small. This stems from the fact that splitting of a multiplet of degenerate states does not affect the position of the centre of gravity of the multiplet (although one should note that in the case of matrix recursion considered above this statement applies to the multiplet of squares of eigenvalues given by equations (5) and (19) rather than to the multiplet of eigenvalues themselves). The conclusion about the relative insignificance of effects associated with the matrix character of the potential [13, 15] is therefore applicable only to the case where the number N_d of d electrons per atom equals five, and hence in a general case angular forces do contribute to interaction between atoms in a transition metal even at the second-moment level of approximation.

It is probably natural to expect that angular terms associated with direct overlap between 3d orbitals become more significant at close separation between the atoms, and that at larger distances the interaction is relatively well approximated by a simpler angular-independent expression based on equation (26). To take this into account we introduce the ‘*quantum core*’ approximation [24, 25] and write the matrix D_{ij} in the form

$$D_{ij} = \frac{1}{5}\delta_{ij}\mu_2(R) + \left[(i|\hat{H}^\dagger\hat{H}|j) - \overline{(i|\hat{H}^\dagger\hat{H}|j)} \right], \quad (29)$$

where the radial functions entering the term in square brackets have shorter range than the function $\mu_2(R)$. In the examples considered below we also used an additional simplifying assumption that the Slater–Koster hopping integrals $(dd\sigma)$, $(dd\pi)$ and $(dd\delta)$ scale as 2:–1:0 and hence

$$D_{ij}(\theta, \phi, R) = \frac{1}{5}\delta_{ij}\mu_2(R) + \left[\mathcal{D}_{ij}(\theta, \phi) - \frac{3}{10}\delta_{ij} \right] g(R). \quad (30)$$

In this case the 15 independent elements of the matrix \mathcal{D}_{ij} have the form

$$\begin{aligned}
\mathcal{D}_{xy,xy} &= \frac{1}{4}(l^2 + m^2 + 8l^2m^2) \\
\mathcal{D}_{xy,yz} &= \frac{1}{4}ln(1 + 8m^2) \\
\mathcal{D}_{xy,xz} &= \frac{1}{4}mn(1 + 8l^2) \\
\mathcal{D}_{xy,x^2-y^2} &= lm(l^2 - m^2) \\
\mathcal{D}_{xy,3z^2} &= \frac{\sqrt{3}}{2}lm(n^2 - l^2 - m^2) \\
\mathcal{D}_{yz,yz} &= \frac{1}{4}(m^2 + n^2 + 8m^2n^2) \\
\mathcal{D}_{yz,zx} &= \frac{1}{4}lm(1 + 8n^2) \\
\mathcal{D}_{yz,x^2-y^2} &= mn \left[l^2 - m^2 - \frac{1}{4} \right] \\
\mathcal{D}_{yz,3z^2} &= \frac{\sqrt{3}}{4}mn [3n^2 - (l^2 + m^2)] \\
\mathcal{D}_{zx,zx} &= \frac{1}{4}(n^2 + l^2 + 8n^2l^2) \\
\mathcal{D}_{zx,x^2-y^2} &= nl \left(l^2 - m^2 + \frac{1}{4} \right) \\
\mathcal{D}_{zx,3z^2} &= \frac{\sqrt{3}}{4}ln [3n^2 - (l^2 + m^2)] \\
\mathcal{D}_{x^2-y^2,x^2-y^2} &= \frac{(l^2 - m^2)^2}{2} + \frac{(l^2 + m^2)}{4} \\
\mathcal{D}_{x^2-y^2,3z^2} &= \frac{\sqrt{3}}{4}(l^2 - m^2) [n^2 - l^2 - m^2] \\
\mathcal{D}_{3z^2,3z^2} &= \frac{1}{4} [4n^4 - n^2(l^2 + m^2) + (l^2 + m^2)^2].
\end{aligned} \tag{31}$$

In the limiting case where $g(R) = 0$ formula (29) gives energies and forces identical to those of the Finnis–Sinclair potential model [3]. The short-range angular-dependent core term in equation (29) can be used to improve the values of formation energies of interstitial atom defects predicted by the model.

The numerical implementation of the quantum core approximation is relatively straightforward. In the case of vanadium (where each atom has four d electrons) the first (radial) part of equation (30) is represented by the embedding part of the Ackland–Thetford parametrization [5] of the Finnis–Sinclair model. The radial behaviour of the short-range correction to the Finnis–Sinclair model is approximated by a core term

$$f(R) = \left(1 - \frac{R}{R_0}\right)^3 \left[A_0 + A_1 \left(1 - \frac{R}{R_0}\right) \right], \quad R < R_0.$$

The cut-off radius of the core term, $R_0 = 2.58 \text{ \AA}$, is chosen in such a way that the presence of this term does not affect the equilibrium properties of the original potential (for example, the original fitted values of elastic constants of the Ackland–Thetford parametrization [5] are not influenced by the core term). The coefficients A_0 and A_1 of the pairwise part of the potential, the radial embedding part, and the angular-dependent part are chosen to provide the best fit to the values of defect formation energies found using density functional calculations.

$$\begin{aligned}
A_0^{(\text{pair})} &= 64.475\,066\,086\,1573 \text{ eV \AA}^6 \\
A_1^{(\text{pair})} &= -187.475\,864\,392\,667 \text{ eV \AA}^6 \\
A_0^{(\text{isotr})} &= 78.297\,828\,239\,0324 \text{ eV}^2 \text{ \AA}^6 \\
A_1^{(\text{isotr})} &= 79.793\,162\,857\,1741 \text{ eV}^2 \text{ \AA}^6 \\
A_0^{(\text{angular})} &= -145.372\,669\,797\,215 \text{ eV}^2 \text{ \AA}^6 \\
A_1^{(\text{angular})} &= 229.737\,328\,736\,310 \text{ eV}^2 \text{ \AA}^6.
\end{aligned} \tag{32}$$

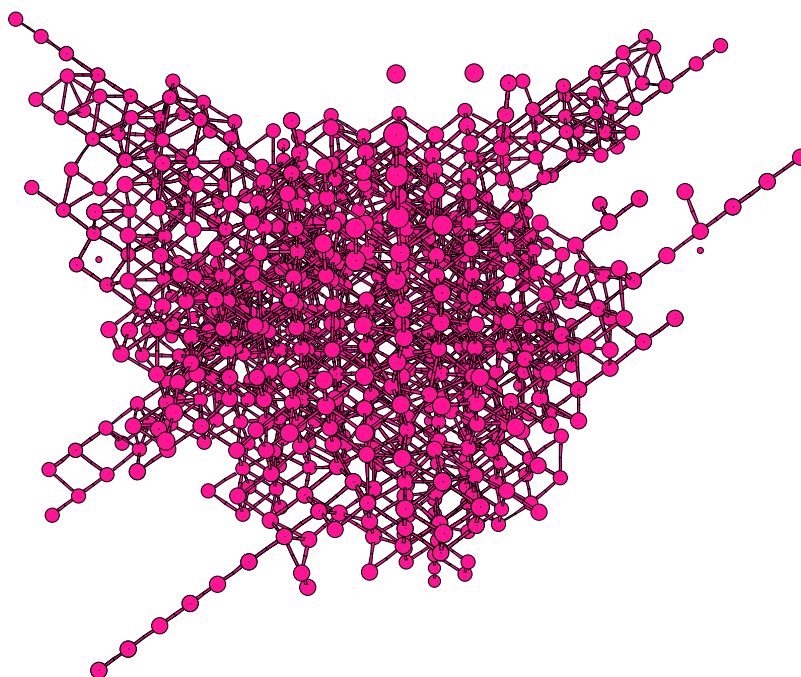


Figure 2. Snapshot of a simulated 380 eV cascade in vanadium taken at $t = 0.33$ ps after the initial impact of an energetic neutron on an atom. This simulation, involving 265 302 atoms, was performed using the matrix potential molecular dynamics algorithm in the quantum core approximation. Atoms shown in this figure have a potential energy that is 0.1 eV higher than the average potential energy of atoms in a perfect lattice. The remaining atoms in the simulation cell are not shown, although interaction between *all* the atoms was taken into account when evaluating energies and interatomic forces. The figure illustrates the feasibility of performing large-scale molecular-dynamics simulations of radiation damage using the matrix potentials.

(This figure is in colour only in the electronic version)

The energies of several configurations of a self-interstitial atom defect evaluated using the quantum core approximation (30) are given in table 1. Asterisks indicate cases where defect configurations were found to be asymptotically unstable and decayed into lower-energy configurations under the influence of thermal fluctuations. Values of formation energies of the octahedral and the tetrahedral configurations were not used in the fitting procedure.

The defect formation energies given in table 1 show that the inclusion of angular terms in the formalism does improve the agreement between the semi-empirical potential approach, which in this work is taken in the matrix form, and first-principles electronic structure calculations. The fact that the matrix elements of D_{ij} have the relatively simple form (31), and hence can be differentiated analytically to find forces acting between atoms, makes the matrix potential method suitable for a fairly large-scale atomistic simulation. To illustrate the point, we consider an example of a simulation that so far has never been performed using a method based on matrix diagonalization.

Figure 2 shows a snapshot of a 380 eV collision cascade in vanadium initiated by an impact of an energetic particle (for example, a neutron) on an atom near the centre of the simulation cell. The snapshot corresponds to the moment approximately 0.33 ps after the initial impact. The simulation was performed using a cell containing 265 302 atoms, and the simulation algorithm used equations (7) and (24). This test showed that the computational

Table 1. Calculated formation energies of various self-interstitial atom configurations.
* corresponds to a locally unstable configuration.

Defect configuration	E_f (eV)		E_f (eV)	
	DFT [8]	[5]	[29]	present QC
111	3.14	4.58	3.27	3.14
110	3.48	4.14	3.66	3.48
100	3.57	4.79	3.60	3.57
Octahedral	3.62	4.77	3.60*	3.56
Tetrahedral	3.69	4.75	3.64	3.81*

speed of the matrix potential algorithm (in the quantum core approximation) was approximately equal to one-third of the speed of a conventional algorithm where forces are evaluated using a spherically symmetric many-body potential (in this case it is the Ackland–Thetford potential for vanadium [5]). The results of this test show that the matrix potential approach described in this paper offers a relatively simple recipe for including angular terms, consistent with the symmetry of the underlying picture of d–d bonding, in a large-scale molecular dynamics simulation of radiation damage.

Acknowledgments

The author gratefully acknowledges many stimulating discussions with Professor Marshall Stoneham FRS. This work has benefited from discussions with Professors David Pettifor FRS and Adrian Sutton FRS. The author is grateful to Dr Peter Derlet for highlighting the significance of the matrix as opposed to the scalar recursion treatment of interatomic interactions. The author acknowledges a comment by Professor Georges Martin, who noted the similarity between equation (22) and the Hellmann–Feynman theorem.

The author would like to thank Drs I Cook and J W Connor for reading the manuscript and for helpful comments. Work at the UKAEA Culham Science Centre was supported by the UK Engineering and Physical Sciences Research Council (EPSRC), the EXTREMAT integrated project, and by EURATOM.

Appendix A

The matrix elements including contributions of $(dd\sigma)$, $(dd\pi)$, and $(dd\delta)$ overlap have the form

$$\begin{aligned}
(xy|\hat{H}^\dagger\hat{H}|xy) &= 3l^2m^2(dd\sigma)^2 + (l^2 + m^2 - 4l^2m^2)(dd\pi)^2 + (n^2 + l^2m^2)(dd\delta)^2 \\
(xy|\hat{H}^\dagger\hat{H}|yz) &= 3lm^2n(dd\sigma)^2 + ln(1 - 4m^2)(dd\pi)^2 + ln(m^2 - 1)(dd\delta)^2 \\
(xy|\hat{H}^\dagger\hat{H}|xz) &= 3l^2mn(dd\sigma)^2 + mn(1 - 4l^2)(dd\pi)^2 + mn(l^2 - 1)(dd\delta)^2 \\
(xy|\hat{H}^\dagger\hat{H}|x^2 - y^2) &= \frac{3}{2}lm(l^2 - m^2)(dd\sigma)^2 + 2lm(m^2 - l^2)(dd\pi)^2 + \frac{1}{2}lm(l^2 - m^2)(dd\delta)^2 \\
(xy|\hat{H}^\dagger\hat{H}|3z^2 - r^2) &= \sqrt{3}lm[n^2 - \frac{1}{2}(l^2 + m^2)](dd\sigma)^2 - 2\sqrt{3}lmn^2(dd\pi)^2 \\
&\quad + \frac{\sqrt{3}}{2}lm(1 + n^2)(dd\delta)^2 \\
(yz|\hat{H}^\dagger\hat{H}|yz) &= 3m^2n^2(dd\sigma)^2 + (m^2 + n^2 - 4m^2n^2)(dd\pi)^2 + (l^2 + m^2n^2)(dd\delta)^2 \\
(yz|\hat{H}^\dagger\hat{H}|xz) &= 3n^2lm(dd\sigma)^2 + lm(1 - 4n^2)(dd\pi)^2 + lm(n^2 - 1)(dd\delta)^2 \\
(yz|\hat{H}^\dagger\hat{H}|x^2 - y^2) &= \frac{3}{2}mn(l^2 - m^2)(dd\sigma)^2 - mn[1 + 2(l^2 - m^2)](dd\pi)^2 \\
&\quad + mn[1 + \frac{1}{2}(l^2 - m^2)](dd\delta)^2
\end{aligned}$$

$$\begin{aligned}
(yz|\hat{H}^\dagger\hat{H}|3z^2-r^2) &= \sqrt{3}mn\left[n^2-\frac{1}{2}(l^2+m^2)\right](dd\sigma)^2 + \sqrt{3}mn(l^2+m^2-n^2)(dd\pi)^2 \\
&\quad - \frac{\sqrt{3}}{2}mn(l^2+m^2)(dd\delta)^2 \\
(xz|\hat{H}^\dagger\hat{H}|xz) &= 3n^2l^2(dd\sigma)^2 + (n^2+l^2-4n^2l^2)(dd\pi)^2 + (m^2+n^2l^2)(dd\delta)^2 \\
(xz|\hat{H}^\dagger\hat{H}|x^2-y^2) &= \frac{3}{2}nl(l^2-m^2)(dd\sigma)^2 + nl\left[1-2(l^2-m^2)\right](dd\pi)^2 \\
&\quad - nl\left[1-\frac{1}{2}(l^2-m^2)\right](dd\delta)^2 \\
(xz|\hat{H}^\dagger\hat{H}|3z^2-r^2) &= \sqrt{3}ln\left[n^2-\frac{1}{2}(l^2+m^2)\right](dd\sigma)^2 + \sqrt{3}ln(l^2+m^2-n^2)(dd\pi)^2 \\
&\quad - \frac{\sqrt{3}}{2}ln(l^2+m^2)(dd\delta)^2 \\
(x^2-y^2|\hat{H}^\dagger\hat{H}|x^2-y^2) &= \frac{3}{4}(l^2-m^2)^2(dd\sigma)^2 + [l^2+m^2-(l^2-m^2)^2](dd\pi)^2 \\
&\quad + \left[n^2+\frac{1}{4}(l^2-m^2)^2\right](dd\delta)^2 \\
(x^2-y^2|\hat{H}^\dagger\hat{H}|3z^2-r^2) &= \frac{\sqrt{3}}{2}(l^2-m^2)\left[n^2-\frac{1}{2}(l^2+m^2)\right](dd\sigma)^2 \\
&\quad + \sqrt{3}n^2(m^2-l^2)(dd\pi)^2 + \frac{\sqrt{3}}{4}(1+n^2)(l^2-m^2)(dd\delta)^2 \\
(3z^2-r^2|\hat{H}^\dagger\hat{H}|3z^2-r^2) &= \left[n^2-\frac{1}{2}(l^2+m^2)\right]^2(dd\sigma)^2 + 3n^2(l^2+m^2)(dd\pi)^2 \\
&\quad + \frac{3}{4}(l^2+m^2)^2(dd\delta)^2.
\end{aligned}$$

Appendix B. The sd-model

In the case where sub-bands of 3d and 4s states both contribute to bonding between atoms, the additional s-d elements of the matrix $\hat{H}^\dagger\hat{H}$ have the form

$$\begin{aligned}
(s|\hat{H}^\dagger\hat{H}|s) &= (ss\sigma)^2 \\
(s|\hat{H}^\dagger\hat{H}|xy) &= \sqrt{3}lm(sd\sigma)[(dd\sigma) + (ss\sigma)] \\
(s|\hat{H}^\dagger\hat{H}|xz) &= \sqrt{3}ln(sd\sigma)[(dd\sigma) + (ss\sigma)] \\
(s|\hat{H}^\dagger\hat{H}|yz) &= \sqrt{3}mn(sd\sigma)[(dd\sigma) + (ss\sigma)] \\
(s|\hat{H}^\dagger\hat{H}|x^2-y^2) &= \frac{\sqrt{3}}{2}(l^2-m^2)(sd\sigma)[(dd\sigma) + (ss\sigma)] \\
(s|\hat{H}^\dagger\hat{H}|3z^2-r^2) &= \frac{1}{2}(3n^2-1)(sd\sigma)[(dd\sigma) + (ss\sigma)] \\
&= \left[n^2-\frac{1}{2}(l^2+m^2)\right](sd\sigma)[(dd\sigma) + (ss\sigma)].
\end{aligned}$$

References

- [1] Stoneham A M, Matthews J R and Ford I J 2004 *J. Phys.: Condens. Matter* **16** S2597
- [2] Matthews J R, Stoneham A M and Ford I J 1999 Future directions for fusion power plant materials modelling in the UK *EURATOM/UKAEA Fusion Association Report* unpublished
- [3] Finnis M W and Sinclair J E 1984 *Phil. Mag.* A **50** 45
Finnis M W and Sinclair J E 1986 *Phil. Mag.* A **53** 161
- [4] Finnis M W 2003 *Interatomic Forces in Condensed Matter* (Oxford: Oxford University Press) p 230
- [5] Ackland G J and Thetford R 1987 *Phil. Mag.* A **56** 15
- [6] Daw M S and Baskes M I 1983 *Phys. Rev. Lett.* **50** 1285
Daw M S and Baskes M I 1984 *Phys. Rev.* B **29** 6443

- [7] Domain C and Becquart C S 2001 *Phys. Rev. B* **65** 024103
- [8] Han S, Zepeda-Ruiz L A, Ackland G J, Car R and Srolovitz D J 2002 *Phys. Rev. B* **66** 220101
- [9] Fu C-C, Willaime F and Ordejón P 2004 *Phys. Rev. Lett.* **92** 175503
- [10] Nguyen-Manh D, Horsfield A and Dudarev S L 2006 *Phys. Rev. B* **73** 020101
- [11] Mendeleev M I, Han S, Srolovitz D J, Ackland G J, Sun D Y and Asta M 2003 *Phil. Mag.* **83** 3977
- [12] Zepeda-Ruiz L A, Han S, Srolovitz D J, Car R and Wirth B D 2003 *Phys. Rev. B* **67** 134114
- [13] Carlsson A E 1991 *Phys. Rev. B* **44** 6590
- [14] Kress J D and Voter A F 1991 *Phys. Rev. B* **43** 12607
- [15] Foiles S M 1993 *Phys. Rev. B* **48** 4287
- [16] Pettifor D G and Aoki M 1991 *Phil. Trans. R. Soc. A* **334** 439
- [17] Pettifor D G 1995 *Bonding and Structure of Molecules and Solids* (Oxford: Oxford University Press)
- [18] Krasko G L, Rice B and Yip S 1999 *J. Comput.-Aided Mater. Des.* **6** 129
- [19] Inoue J and Ohta Y 1987 *J. Phys. C: Solid State Phys.* **20** 1947
- [20] Ozaki T, Aoki M and Pettifor D G 2000 *Phys. Rev. B* **61** 7972
- [21] Landau L D and Lifshits E M 1977 *Quantum Mechanics, Non-Relativistic Theory* 3rd edn (Oxford: Pergamon) pp 138–42
- [22] Pettifor D G and Weaire D L (ed) 1984 *The Recursion Method and Its Applications Proc. Conf. (Imperial College, London, Sept. 1984)* (Berlin: Springer)
- [23] Horsfield A P, Bratkovsky A M, Pettifor D G and Aoki M 1996 *Phys. Rev. B* **53** 1656
- [24] Dudarev S L 2004 *J. Nucl. Mater.* **329–333** 1151
- [25] Dudarev S L 2004 *Proc. 2nd Int. Conf. on Multiscale Materials Modelling* ed N Ghoniem (Los Angeles, CA: UCLA Press) pp 492–5
- [26] Sutton A P 1993 *Electronic Structure of Materials* (Oxford: Oxford University Press) pp 174–82
- [27] Slater J C and Koster G F 1954 *Phys. Rev.* **94** 1498
- [28] Feynman R P 1939 *Phys. Rev.* **56** 340
- [29] Han S, Zepeda-Ruiz L A, Ackland G J, Car R and Srolovitz D J 2003 *J. Appl. Phys.* **93** 3328